*Eur. J. Biochem.* **270**, 4478–4487 (2003) © FEBS 2003 doi:10.1046/j.1432-1033.2003.03840.x

# Bilayer localization of membrane-active peptides studied in biomimetic vesicles by visible and fluorescence spectroscopies

**Tanya Sheynis[1], Jan Sykora[2], Ales Benda[2], Sofiya Kolusheva[1], Martin Hof[2] and Raz Jelinek[1]**

[1]*Department of Chemistry and the Stadler Minerva Center for Mesoscopic Macromolecular Engineering, Ben Gurion University of the Negev, Beersheva, Israel;* [2]*J. Heyrovsky Institute of Physical Chemistry, Academy of Sciences of the Czech Republic, and Center for Complex Molecular Systems and Biomolecules, Prague, the Czech Republic*

Depth of bilayer penetration and effects on lipid mobility conferred by the membrane-active peptides magainin, melittin, and a hydrophobic helical sequence $KKA(LA)_7KK$ (denoted KAL), were investigated by colorimetric and time-resolved fluorescence techniques in biomimetic phospholipid/poly(diacetylene) vesicles. The experiments demonstrated that the extent of bilayer permeation and peptide localization within the membrane was dependent upon the bilayer composition, and that distinct dynamic modifications were induced by each peptide within the head-group environment of the phospholipids. Solvent relaxation, fluorescence correlation spectroscopy and fluorescence quenching analyses, employing probes at different locations within the bilayer, showed that magainin and melittin inserted close to the glycerol residues in bilayers incorporating negatively charged phospholipids, but predominant association at the lipid–water interface occurred in bilayers containing zwitterionic phospholipids. The fluorescence and colorimetric analyses also exposed the different permeation properties and distinct dynamic influence of the peptides: magainin exhibited the most pronounced interfacial attachment onto the vesicles, melittin penetrated more into the bilayers, while the KAL peptide inserted deepest into the hydrophobic core of the lipid assemblies. The solvent relaxation results suggest that decreasing the lipid fluidity might be an important initial factor contributing to the membrane activity of antimicrobial peptides.

*Keywords*: solvent relaxation; fluorescence correlation spectroscopy; lipid bilayers; poly(diacetylene); biomimetic membranes.

The emergence of bacterial strains resistant to conventional antibiotics is a major cause of inefficient therapy and increased mortality from bacterial infection. The use of antimicrobial peptides as a therapeutic tool has been among the most promising avenues investigated, to date, for addressing antibiotic resistance. Antimicrobial peptides, mostly cationic and amphipathic amino acid sequences, are found in all living species and are produced in large quantities at sites of infection and/or inflammation [1]. These peptides generally function without either high specificity or memory [1,2]. Varied approaches have been presented, aiming to decipher the mode of action of antimicrobial peptides and their specificity towards bacterial rather than host cells; however, the exact mechanisms by which these peptides kill bacteria are still not fully understood. Several studies have shown that peptide–lipid interactions leading to membrane permeation play major roles in the activities of antimicrobial peptides [3–5].

Two main structural models have been developed, in recent years, correlating membrane disruption activities and antimicrobial peptide–membrane interactions. One model describes a mechanism of *trans*-membrane pore formation via a 'barrel-stave' organization [6], while a second model, denoted the 'carpet mechanism', proposes accumulation of the amphipathic peptides at the membrane interface as the main determinant of cell destruction through membrane micellization or formation of transient pores [4,7]. An important determinant for both models concerns the extent of peptide permeation into the lipid bilayer and the localization of the membrane-associated peptides within the bilayer. Even though a large body of published data exists pertaining to membrane interaction properties of antimicrobial peptides, there are only a limited number of studies in which the exact bilayer localization and depth of peptide penetration were analysed. The aims of the present study were to investigate the bilayer penetration

*Correspondence to* R. Jelinek, Department of Chemistry and the Stadler Minerva Center for Mesoscopic Macromolecular Engineering, Ben Gurion University of the Negev, Beersheva 84105, Israel.
Fax: + 972 8 6472943, Tel.: + 972 8 6461747,
E-mail: razj@bgumail.bgu.ac.il

*Abbreviations*: %CR, percentage colorimetric response; KAL, peptide sequence KKA(LA)7KK; NBD-PE, *N*-(7-nitrobenz-2-oxa-1,3-diazol-4-yl)1,2-dihexadecanoyl-*sn*-glycero-3-phosphoethanolamine, triethylammonium salt; $Ole_2$PtdCho, dioleoylphosphatidylcholine; $Ole_2$PtdSer, dioleoylphosphatidylserine; Patman, 6-hexadecanoyl-2-(((2-(trimethylammonium)ethyl)methyl)amino)-naphthalene chloride; PDA, poly(diacetylene); PamOlePtdCho, palmitoyloleylphosphatidylcholine; Rhodamine Red–DHPE, Rhodamine Red™–X-1,2-dihexadecanoyl-*sn*-glycero-3-phosphoethanolamine, triethylammonium salt; SR, solvent relaxation; SUV, small unilamellar vesicles; TRES, time-resolved emission spectra.

(Received 30 June 2003, revised 1 September 2003, accepted 18 September 2003)

depth of three representative membrane peptides and to determine their effects on the lipid dynamics. Specifically, the experiments were designed to probe the roles of negatively charged phospholipids, relatively abundant within bacterial membranes, to determine peptide binding and membrane permeation.

The peptides investigated here were magainin-II [5,8,9], melittin [3,4,10,11], and a hydrophobic membrane-spanning synthetic sequence $KKA(LA)_7KK$ [12,13] (single letter amino acid code; the peptide is denoted 'KAL'). Magainin is a cationic amphipatic peptide, known to be highly effective in killing Gram-negative bacteria [14,15]. Previous studies have pointed to a preferred localization of magainin at membrane surfaces [5,16,17]. Melittin is a widely studied helical cationic peptide that exhibits non-cell-specific lytic properties [3,8,10]. Membrane permeation, induced by melittin, has been investigated using different techniques and is believed to be related to interface association followed by pore formation/membrane micellization processes [18–20]. The highly hydrophobic sequence, KAL, is a transmembrane helical peptide known to vertically span lipid bilayers [12,13]. We have previously demonstrated that KAL is incorporated within lipid bilayers in mixed lipid/poly(diacetylene) (PDA) vesicles, allowing the surface display of peptide epitopes attached to its N-terminus [21].

Analysis of peptide–lipid interactions was carried out in the present study through a combination of colorimetric and advanced fluorescence spectroscopy techniques, employing probes incorporated within phospholipid bilayers in lipid/polymer vesicles (Fig. 1). The choice of the biomimetic lipid/PDA vesicle assay as a platform for studying membrane processes was based upon the unique biochromatic properties of the mixed vesicles [22,23], allowing their application as a useful tool for evaluation of peptide binding and penetration into lipid bilayers. The lipid/PDA assembly was previously shown to organize in biomimetic bilayer domains and the assay has been used for studying diverse membrane processes [21,23–29]. Importantly, we have shown that the presence of the PDA matrix within phospholipid/PDA vesicles does not interfere with peptide–lipid interactions in these systems, and that nonspecific interactions of membrane peptides with the PDA moieties in the mixed assemblies are minimal [26,29].

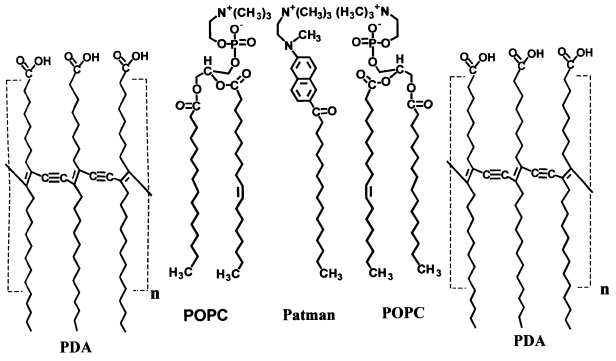


**Fig. 1. Schematic structure of a vesicle surface containing the fluorescent dye 6-hexadecanoyl-2-(((2-(trimethylammonium)ethyl)methyl) amino)-naphthalene chloride (Patman).** The scheme depicts a fraction of the phospholipid–poly(diacetylene) (PDA) bilayer surface model used in this study. The picture shows the PDA framework (parts of the repeating polymer units are indicated; the conjugated ene-yne backbone spans the entire polymerized PDA structure); phospholipids (PamOlePtdCho or $Ole_2$PtdSer/PamOlePtdCho); and Patman embedded within the phospholipid assembly. Note the proximity of the fluorescent moiety of Patman to the glycerol groups of the phospholipids.

Solvent-relaxation (SR), the primary spectroscopic method employed in this study, is a recently developed sensitive fluorescence technique used for probing relative penetration of molecular species into lipid bilayers and investigating their dynamic effects [30,31]. Recent studies have demonstrated that suitable fluorescent dyes located within either the hydrophilic headgroup region or the hydrophobic core of lipid bilayers facilitate direct observation of viscosity and polarity changes at the local environments of the probes [32–35]. Here we measured the effects of membrane peptides upon the SR of the fluorescent dye 6-hexadecanoyl-2-(((2-(trimethylammonium)ethyl)methyl) amino)-naphthalene chloride (Patman) [33,36–38], incorporated in the vicinity of the glycerol interface within the phospholipid domains in the lipid/PDA vesicles (Fig. 1). This work is one of the first methodical studies to examine lipid bilayer permeation by membrane-active peptides through application of SR.

Additional fluorescence experiments, which complemented the SR analysis, included fluorescence quenching of a lipid-surface probe, *N*-(7-nitrobenz-2-oxa-1,3-diazol-4-yl)1,2-dihexadecanoyl-*sn*-glycero-3-phosphoethanolamine (NBD-PE) [39], and fluorescence correlation spectroscopy employing 1,2-dihexadecanoyl-*sn*-glycero-3-phosphoethanolamine, triethylammonium salt (Rhodamine Red-DHPE) incorporated within planar phospholipid bilayers. We also examined the relative depth of peptide insertion into negative and zwitterionic lipid bilayers by comparing the dose–response curves of the colorimetric transitions induced by the peptides within the phospholipid/PDA vesicles.

## Materials and methods

### Materials

Phospholipids, including palmitoyloleoylphosphatidylcholine (PamOlePtdCho), dioleoylphosphatidylcholine ($Ole_2$PtdCho) and dioleoylphosphatidylserine ($Ole_2$PtdSer) were purchased from Sigma-Aldrich Co. (St Louis, MO, USA). The diacetylenic monomer, 10,12-tricosadiynoic acid, was purchased from GFS Chemicals (Powell, OH, USA), washed in chloroform, and filtered through a 0.45-μm filter prior to use. Fluorescent probes 6-palmitoyl (trimethylammoniumethyl) methylamino naphthalene chloride (Patman), *N*-(7-nitrobenz-2-oxa-1,3-diazol-4-yl)1,2-dihexadecanoyl-*sn*-glycero-3-phosphoethanolamine, triethylammonium salt (NBD-PE) and Rhodamine Red™-X-1,2-dihexadecanoyl-*sn*-glycero-3-phosphoethanolamine, triethylammonium salt (Rhodamine Red-DHPE) were purchased from Molecular Probes (Leiden, the Netherlands).

### Peptides

Melittin (GIGAVLKVLTTGLPALISWIKRKRQQ), magaininII (GIGKFLHSAKKFGKAFVGEIMNS) and

KAL were synthesized using solid-phase peptide synthesis and purified to > 97% using reverse-phase HPLC. Purity of the peptides was confirmed with amino acid analysis and analytical HPLC.

### Vesicle preparation

All lipid constituents were dissolved in chloroform/ethanol (1 : 1, v/v) and dried *in vacuo* to constant weight. Apart from vesicle preparations for fluorescence correlation spectroscopy measurements (see below), all lipid films were suspended in deionized water, followed by probe sonication on a Misonix Incorporated sonicator (Farmingdale, NY, USA), applying an output power of ≈100 W. Vesicles containing lipid components and PDA (PamOlePtdCho/PDA, 2 : 3 molar ratio; $Ole_2$PtdSer/PamOlePtdCho/PDA, 1 : 1 : 3 molar ratio) were sonicated at 70 °C for 3–4 min. The vesicle suspensions were then cooled to room temperature, incubated overnight at 4 °C, and polymerized by irradiation at 254 nm for 20–30 s, resulting in solutions with an intense blue appearance. Small unilamellar vesicles (SUVs), composed of the phospholipids PamOlePtdCho and $Ole_2$PtdSer/PamOlePtdCho (1 : 1 molar ratio) were prepared through sonication of the aqueous lipid mixtures at room temperature for 9 min. Vesicle suspensions were allowed to anneal for 30 min and centrifuged for 15 min at 6000 ***g*** to remove any titanium particles.

### Ultracentrifugation binding assay

An ultracentrifugation binding assay was carried out for evaluating peptide affinities to the vesicles (partition coefficients [29,40]), in order to obtain an accurate comparison of colorimetric transitions induced by each peptide (see below). First, a calibration graph that correlated peptide concentration with the absorbance at 220 nm was prepared and used to determine the concentration of soluble, unbound peptide. Varying quantities of peptides were added to aqueous lipid/PDA vesicle solutions (≈ 0.2 mM phospholipids in 25 mM Tris base, pH 8.0), and the solutions were incubated briefly at ambient temperature to allow equilibration of bound and unbound peptide species before centrifugation at 30 000 r.p.m. for 40 min in a Beckman 47-65 ultracentrifuge (Beckman Instruments Inc., Fullerton, CA, USA) using an SW-55 rotor to deposit vesicle–peptide aggregates. The concentration of soluble (unbound) peptide in the supernatant was determined by extrapolation from the calibration curve, and the difference from the initial peptide concentration represented the quantity of bound peptide.

### UV-vis measurements

Peptides at concentrations ranging from 1 to 15 μM were added to 60 μl of PDA-containing vesicle solutions consisting of ≈0.2 mM phospholipids in 25 mM Tris-base (pH 8.0). Following addition of the peptides, the solutions were diluted to 1 mL and spectra were acquired at 28 °C, between 400 nm and 700 nm, on a Jasco V-550 spectrophotometer (Jasco Corp., Tokyo, Japan), using a 1-cm optical path cell.

To quantify the extent of blue-to-red color transitions within the vesicle solutions, the percentage colorimetric response (%CR), was defined and calculated as follows [41]:

$$\%\,\mathrm{CR} = \frac{(PB_0 - PB_\mathrm{I})}{PB_0} \times 100$$

where $PB = A_{blue}/(A_{blue} + A_{red})$, and $A$ is the absorbance at 640 nm, the 'blue' component of the spectrum, or at 500 nm, the 'red' component ('blue' and 'red' refer to the visual appearance of the material, not actual absorbance). $PB_0$ is the blue/red ratio of the control sample before induction of a color change, and $PB_\mathrm{I}$ is the value obtained for the vesicle solution after the colorimetric transition occurred.

### SR measurements

Patman was added to the preformed vesicles, from a 2 mM (ethanolic) stock solution, to yield a phospholipid/dye molar ratio of 30 : 1. For PDA-containing vesicles, Patman was added after the polymerization step (see Vesicle preparation, above); probe addition did not affect the colorimetric properties of the vesicles. Fluorescence decays and steady-state spectra were recorded using an IBH 5000 U SPC equipment and a Fluorolog 3 (Jobin-Yvon) steady-state spectrometer, respectively, at 28 °C. Decay kinetics were recorded by using a Picoquant PLS-370 excitation source (378 nm peak wavelength, 0.5 ns pulse width, 5 MHz repetition rate) and a cooled Hamamatsu R3809U-50 microchannel plate photomultiplier. Time-resolved emission spectra (TRES) were calculated from the fit parameters of the multiexponential decays detected from 400 to 530 nm and the corresponding steady-state intensities [42]. The TRES were fitted by log-normal functions [43]. Correlation functions C(t) were calculated from the emission maxima $\nu$(t) of the TRES at a defined time t after excitation:

$$\mathrm{C(t)} = \frac{\nu(\mathrm{t}) - \nu(\infty)}{\nu(0) - \nu(\infty)}$$

where $\nu(0)$ and $\nu(\infty)$ are the emission maxima (in $cm^{-1}$) at times zero and $\infty$, respectively. The time zero spectrum and the corresponding $\nu(0)$ values were determined as described previously [42,44]. The $\nu(\infty)$ values were assessed by inspection of the reconstructed TRES [42]. In all cases, the solvent response cannot be satisfactorily described by a single-exponential relaxation model. In order to characterize the overall timescale of the solvent response, an (integral) average relaxation time was used:

$$\langle \mathrm{t_r} \rangle \equiv \int_\infty^0 \mathrm{C(t)dt}$$

### Fluorescence quenching measurements

NBD-PE was added to lipids from 1 mM chloroform stock solution, yielding a final concentration of 4 μM, then dried together in a vacuum before sonication (see Vesicle preparation, above). Samples were prepared by adding peptides at a 1-μM bound concentration to 60 μL of vesicle solutions at ≈0.2 mM total lipid concentration in 25 mM Tris base (pH 8.0). The quenching reaction was initiated by adding

sodium dithionite from a 0.6 M stock solution, prepared in 50 mM Tris base (pH 11.0) buffer, to a final concentration of 0.6 mM. The decrease in fluorescence was recorded for 210 s at 28 °C using 468 nm excitation and 538 nm emissions on an Edinburgh FL920 spectrofluorimeter. The fluorescence decay was calculated as a percentage of the initial fluorescence measured before the addition of dithionite.

### Fluorescence correlation spectroscopy

In order to determine lateral diffusion coefficients in bilayers, SUVs consisting of $Ole_2$PtdSer/$Ole_2$PtdCho (1 : 4 molar ratio) were prepared as previously described [45]. The vesicles were labeled with Rhodamine Red-DHPE (ratio of labeled to unlabeled lipid 1 : 200 000) and adsorbed onto mica. It has been shown previously that under the experimental conditions used in the present study, planar confluent bilayers are formed [45]. The preparation of those supported phospholipid bilayers consists of cleaning and assembling of microscope borosilicate glass slides (Paul Marienfeld GmbH & Co. KG, Louda-Königshofen, Germany) and mica plates (5 mm in diameter; Methafix, Montdidier, France), application and incubation of the SUVs, and flushing of the redundant SUVs. The exact description of those procedures, and a schematic view of the sample cell, has been published previously [45]. Fluorescence correlation spectroscopy measurements were performed using a Confocor 1 (Carl Zeiss GmbH, Jena, Germany; Evotec Biosystems GmbH, Hamburg, Germany) containing a Helium-Neon laser as the excitation source (543 nm excitation wavelength). The determination of diffusion coefficients was performed employing the newly developed, so-called 'z-scan' approach, which can be briefly summarized as follows [46]. Autocorrelation functions G(τ), calculated from the fluorescence intensity fluctuations, have been determined at different positions along the z-axis in 0.2-μm steps ('z-scans'). The diffusion time, $\tau_D$, in planar systems, depends on the position of the focus of the laser beam with respect to the optical z-axis relative to the phospholipid surface plane. This dependence has been mathematically described by the equation:

$$\tau_D = \frac{w_0^2}{4D}\left(1 + \frac{\lambda_0^2 \Delta z^2}{\pi^2 n^2 w_0^4}\right)$$

where $w_0$ is the radius of the beam in the focal plane, $D$ is the lateral diffusion coefficient, $n$ is the refractive index of medium, λ represents the wavelength of the excitation light, and Δz is the distance between the sample position and the position of beam diameter minimum $z = z_0$. Thus, we performed measurements of autocorrelation functions at different values of Δz and fitted those functions by the equation below yielding the corresponding $\tau_D$ values:

$$G(\tau)_{2DT} = 1 + (1 - T + Te^{-\tau/\tau_{tr}})\left(\frac{1}{PN[1-T]}\right)\left(\frac{1}{1+\tau/\tau_D}\right)$$

where $PN$ and $\tau_D$ represent the particle number and the diffusion time, respectively, $T$ is the average fraction of dye molecules in the triplet state and $\tau_{tr}$ is the intersystem crossing relaxation time. Fitting the dependencies of $\tau_D$ on Δz by the first equation above directly yielded the lateral diffusion coefficient $D$.

## Results

### Depth of bilayer penetration: colorimetric analysis

In order to evaluate the relative depth of peptide penetration into the phospholipid/PDA assemblies, we recorded the colorimetric transitions induced in the vesicle solutions (Fig. 2). Fluorescence measurements carried out in this work (see below) demonstrated a high structural and dynamic similarity between the lipid environments in phospholipid/PDA vesicles and the more conventional unilamellar vesicles that did not contain PDA.

Figure 2 shows graphs corresponding to the %CR (degree of blue–red transition; see the Materials and methods) induced by increasing the quantity of bound peptides, i.e. the extent of induced blue–red transitions affected by the added peptides. The results in Fig. 2 show that the %CR values correlate with the concentrations of vesicle-bound peptides after accounting for the partition coefficients determined by ultracentrifugation binding assays (see the Materials and methods). Therefore, the curves reveal that each peptide interacts with the membrane phospholipids differently, particularly with respect to the degree of penetration into the lipid layer. Furthermore,

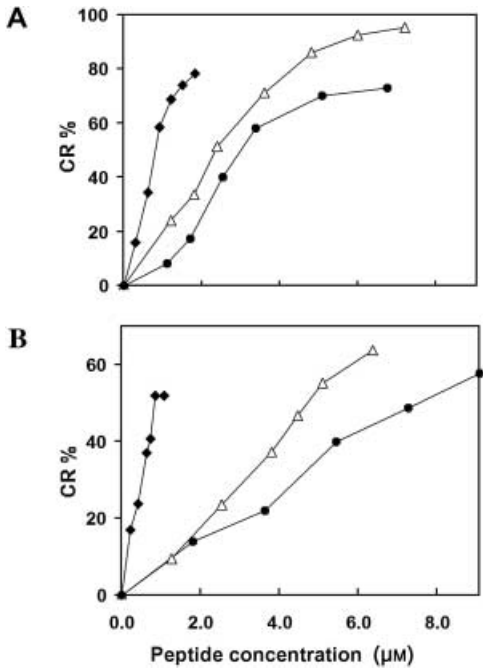


**Fig. 2. Colorimetric transitions induced by peptides in PamOlePtdCho/PDA vesicles and $Ole_2$PtdSer/PamOlePtdCho/PDA vesicles, respectively.** The percentage colorimetric response (%CR, see the Materials and Methods) induced by the peptides in (A) PamOlePtdCho/PDA vesicles and (B) $Ole_2$PtdSer/PamOlePtdCho/PDA vesicles is shown. Peptide symbols are: ●, peptide sequence KKA(LA)7KK (KAL); △, melittin; and ◆, magainin. The colorimetric data indicate differences in lipid bilayer penetration among peptides, as well as dependence upon lipid composition.

Fig. 2 shows that relative peptide insertion depends also upon the vesicle phospholipid composition, i.e. zwitterionic vs. negatively charged phospholipids.

Interfacial lipid perturbation was previously shown to induce a greater increase in %CR as a function of the quantity of bound peptide, while peptides that penetrate deeper into the hydrophobic core of the membrane bilayer produce a lower rise in chromatic shift [26,27,29,47]. In principle, a direct relationship exists between higher %CR and interfacial lipid binding because the mechanism of colorimetric transformation of the polymer assumes an increased mobility of the pendant side-chains, induced through perturbations at the lipid/PDA vesicle surface [22]. In the two lipid systems examined, magainin gave rise to the steepest increases in %CR at peptide concentrations $\leq 2$ μM (Fig. 2). The magainin %CR values were between two and four times higher than those induced by melittin or KAL, an indication that magainin is located predominantly at the lipid–water interface, causing enhanced perturbation in the head-group region of the lipid–polymer assembly [26,29].

Melittin and KAL, on the other hand, inserted deeper into the hydrophobic core of the lipid bilayer and consequently induced lower %CR values (Fig. 2). Previous studies have indicated that melittin is embedded relatively deeply in lipid/PDA vesicle assemblies [29]. Moreover, a melittin diastereomeric analog, in which the helical structure was disrupted, induced a higher %CR owing to its predominant binding at the lipid–water interface [26]. Similarly, the KAL sequence, containing a repeat of the hydrophobic residues alanine and leucine, is expected to adopt a helical structure and to insert into the hydrophobic core of the phospholipid bilayer in a transmembrane orientation [12,13].

Examination of the data in Fig. 2 further indicates that the presence of negatively charged phospholipids within the vesicles promotes deeper insertion of melittin and KAL, but does not seem to affect the strong interfacial binding of magainin. For example, at peptide concentrations of 2 μM, melittin induced a CR of $\approx 20\%$ in $Ole_2$PtdSer/PamOlePtdCho/PDA vesicles, but twice as much in PamOlePtdCho/PDA vesicles. The corresponding values for KAL were $\approx 15\%$ and 30% in $Ole_2$PtdSer/PamOlePtdCho/PDA and PamOlePtdCho/PDA, respectively, indicating a relatively deeper penetration in the vesicles containing negatively charged phospholipids.

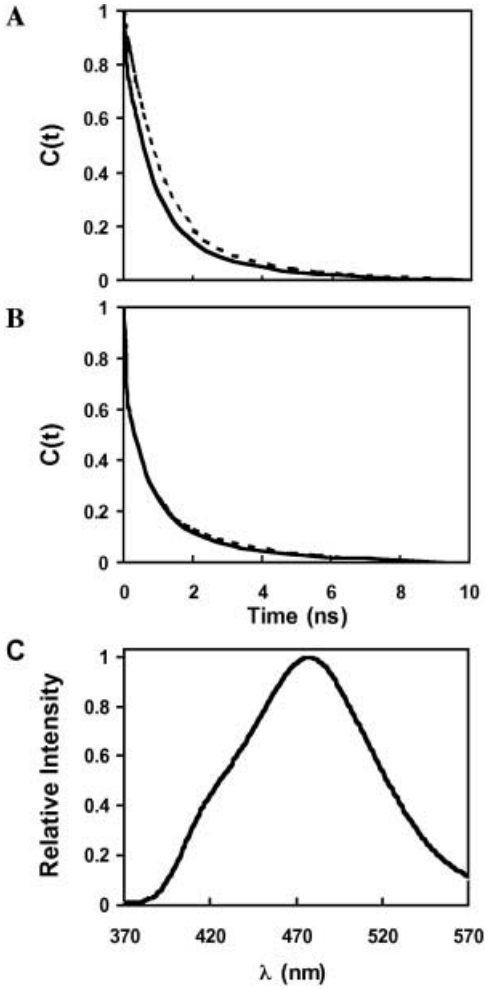


**Fig. 3. Correlation functions and steady state emission spectra of 6-hexadecanoyl-2-(((2-(trimethylammonium)ethyl)methyl)amino)-naphthalene chloride (Patman) in mixed lipid–poly(diacetylene) (PDA) vesicles and vesicles not containing PDA (vesicles comprising phospholipids only).** Correlation functions [C(t)] of Patman are shown in: (A) vesicles containing zwitterionic phospholipids – small unilamellar PamOlePtdCho vesicles (solid curve) and PamOlePtdCho/PDA vesicles (broken curve); and (B) vesicles containing both negative and zwitterionic phospholipids – small unilamellar $Ole_2$PtdSer/PamOlePtdCho vesicles (solid curve) and $Ole_2$PtdSer/PamOlePtdCho/PDA vesicles (broken curve). (C) Steady-state emission spectrum of Patman in PamOlePtdCho/PDA vesicles.

## SR measurements

Additional information on the structural and dynamic consequences of peptide–membrane interactions has been provided by SR analysis using the fluorescent label Patman (Figs 3–5 and Table 1). Patman was previously shown to be located in the vicinity of the glycerol moities in lipid bilayers [35,36] and has been used for probing SR processes within lipid assemblies [33,35,37,38]. Figure 3 compares the SR processes of Patman incorporated in conventional phospholipid SUVs and in the biomimetic phospholipid/PDA assemblies. The traces of the correlation functions C(t) acquired in PamOlePtdCho SUVs and PamOlePtdCho/PDA vesicles (Fig. 3A), or $Ole_2$PtdSer/PamOlePtdCho SUVs and $Ole_2$PtdSer/PamOlePtdCho/PDA vesicles (Fig. 3B), confirm that the presence of the conjugated polymer does not affect the SR properties of Patman. These results also indicate that the phospholipid moieties retain their dynamic properties in the presence of the PDA matrix. Previous data confirmed that lipid molecules adopt microscopic bilayer domains in lipid/PDA assemblies and that the adjacent PDA framework does not perturb the structural or dynamic properties of the lipids [28]. Furthermore, the typical fluorescence emission spectra of Patman were detected only in the presence of phospholipid-containing PDA vesicles (Fig. 3C), and not in pure PDA vesicles (no fluorescence emission from Patman was detected). This result, combined with the data in Fig. 3A,B, confirms that

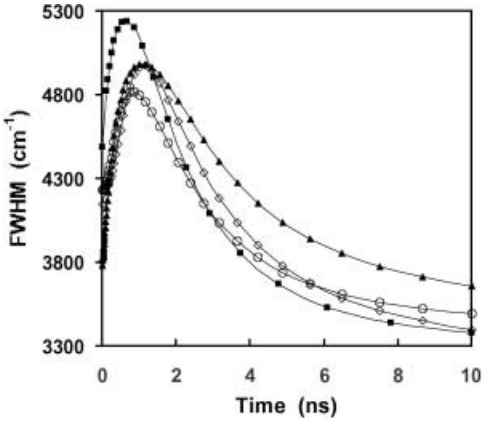


**Fig. 4. Evolution of spectral halfwidths of 6-hexadecanoyl-2-(((2-(trimethylammonium)ethyl)methyl)amino)-naphthalene chloride (Patman) time resolved emission spectra (TRES) after peptide addition to PamOlePtdCho/poly(diacetylene) (PDA) vesicles.** Time evolution profiles are shown of spectral halfwidths (full width at half maximum, fwhm) of the reconstructed TRES of Patman in PamOlePtdCho/PDA vesicles. Curve symbols are: ■, control; ○, peptide sequence KKA(LA)7KK (KAL); ▲, melittin; ◇, magainin.

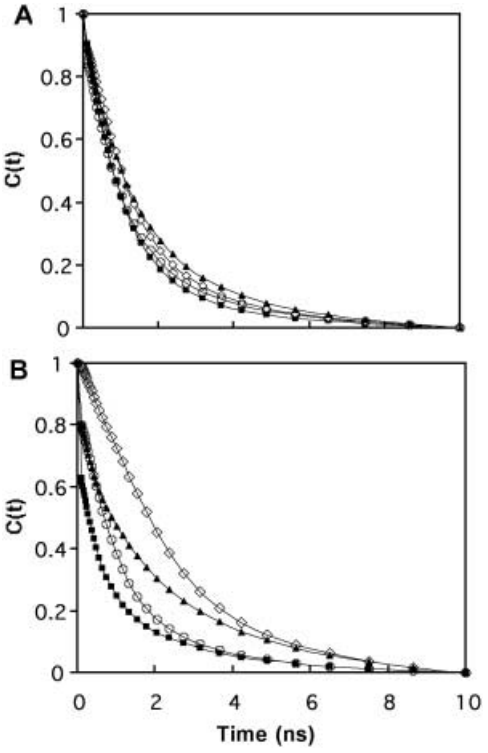


**Fig. 5. Effects on solvent relaxation of 6-hexadecanoyl-2-(((2-(trimethylammonium)ethyl)methyl)amino)-naphthalene chloride (Patman) following addition of peptides.** Correlation function [C($t$)] values of Patman are shown in (A) PamOlePtdCho/poly(diacetylene) (PDA) and (B) $Ole_2$PtdSer/PamOlePtdCho/PDA. Curve symbols are: ■, control; ○, KKA(LA)7KK (KAL); ▲, melittin; ◇, magainin.

the fluorescent label was embedded within the phospholipid domains in the mixed lipid/PDA systems and was excluded from the polymerized matrix.

**Table 1. Solvent relaxation (SR) parameters of Patman in the model vesicles.** KAL, peptide sequence KKA(LA)7KK.

| Vesicle composition | Peptide added | $\tau_r$ (ns)[a] | SR (%)[b] | $\Delta\nu$ ($cm^{-1}$)[c] |
|---|---|---|---|---|
| PamOlePtdCho/PDA | None | 1.3 | 97 | 3480 |
| | KAL | 1.4 | 91 | 3330 |
| | Melittin | 1.7 | 95 | 3310 |
| | Magainin II | 1.6 | 94 | 3290 |
| $Ole_2$PtdSer/PamOlePtdCho/PDA | None | 0.9 | 71 | 3460 |
| | KAL | 1.2 | 85 | 3200 |
| | Melittin | 1.8 | 87 | 3020 |
| | Magainin II | 2.4 | 100 | 3010 |

[a] The average relaxation time was estimated from integration of the correlation function (see text for details). The relative errors in integral relaxation times are below 0.1 ns. [b] Percentage of experimentally determined solvent relaxation [35], obtained by comparison of the $\Delta\nu$ (see [c]) values determined by using the $\nu(0)$ values from the time-zero spectrum estimation with those obtained exclusively by e-resolved emission spectra reconstruction [44]. [c] Time-dependent Stokes shift $\Delta\nu = \nu(0) - \nu(\infty)$. $\nu(0)$ and $\nu(\infty)$ are the emission maxima (in $cm^{-1}$) at times zero and $\infty$, respectively; $\nu(0)$ was determined by time-zero spectrum estimation [44].

Figure 4 depicts representative time evolutions of the TRES of Patman, recorded at full width at half maximum [35,44], following peptide addition to PamOlePtdCho/PDA vesicles. Similar results were obtained for $Ole_2$PtdSer/PamOlePtdCho/PDA vesicles (data not shown). The full width at half maximum curves shown in Fig. 4, both in the case of the control vesicle sample (without addition of peptides) and in the vesicle solutions after addition of each peptide, initially increase and reach maxima at between 1 and 2 ns, followed by an exponential decrease. These profiles confirm that SR is completed during the lifetime of the excited state, and that the SR evolution is almost completely captured by the experimental apparatus employed here, providing subnanosecond time resolution [35].

The effects of peptide–lipid interactions upon the SR of Patman are presented in Fig. 5; the average relaxation times calculated from integration of the curves are summarized in Table 1. The percentage SR values outlined in Table 1 confirm that practically the entire SR processes are recorded in the experiments. Two effects are apparent in Fig. 5 and Table 1. First, significant differences are observed between the two vesicle models. Specifically, while the SR of Patman was only minimally affected by peptide association onto PamOlePtdCho/PDA vesicles (Fig. 5A), in $Ole_2$PtdSer/PamOlePtdCho/PDA the SR clearly slowed down as a result of peptide interactions (Fig. 5B). Furthermore, there appeared to be a distinct effect of each peptide upon the correlation function C(t) of Patman in the $Ole_2$PtdSer/PamOlePtdCho/PDA assembly (Fig. 5B). In particular, the relaxation time increased in the order KAL < melittin < magainin (Table 1), similar to the order observed for the colorimetric responses depicted in Fig. 2.

Table 1 underlies the influence of the three peptides upon the SR of Patman and the dependence of the SR modification upon lipid composition. The significance of lipid

binding and bilayer perturbation are apparent from the relative increase in relaxation time induced by each peptide. Magainin induced the most pronounced dynamic effect in the $Ole_2$PtdSer/PamOlePtdCho/PDA assembly, increasing the relaxation time from 0.9 ns in the control sample to 2.4 ns. Melittin also a induced slower relaxation (1.8 ns, Table 1), albeit to a lesser extent compared with magainin. KAL, on the other hand, gave an SR of 1.2 ns (Table 1) which is the smallest increase in relaxation time.

The time-dependent Stokes shifts of the fluorescent emission of Patman, recorded after peptide addition (Table 1) complement the colorimetric and SR analyses. The time-dependent Stokes shift is related to the polarity of the microenvironment of the fluorescent probe [32,35]. Previous studies have demonstrated that the time-dependent Stokes shifts of Patman in bilayer systems were affected by the micropolarity of its environment [33,36]. The Stokes shift values depicted in Table 1 show different peptide effects in the two vesicle models employed in this work. In the PamOlePtdCho/PDA system, all peptides induced almost the same Stokes shifts (differences among the peptides are $< 200$ cm$^{-1}$), indicating a very small modification of the micropolarity around the fluorescent probe [35]. In the negatively charged vesicle assembly, however, the differences between Stokes shifts were more pronounced, in particular after addition of melittin and magainin (shifts of 440 cm$^{-1}$ and 450 cm$^{-1}$, respectively, in comparison to the control sample, where no peptide was added, Table 1). These shifts, together with the observed slowing down of the SR kinetics induced by both peptides, might correspond to ejection of water molecules around the fluorescent label as well as reduced mobility of the phospholipid interface region.

## Fluorescence correlation spectroscopy

Fluorescence correlation spectroscopy data employing a surface fluorescent probe, Rhodamine Red-DHPE, are summarized in Table 2 and support the interpretation of the SR and colorimetric results. The fluorescence correlation spectroscopy experiments yielded the diffusion rates of DHPE labeled at the headgroup with rhodamine, embedded in a bilayer plane consisting of $Ole_2$PtdSer/$Ole_2$PtdCho adsorbed onto a mica surface. The fluorescence correlation spectroscopy analysis indicates that KAL did not modify the diffusion coefficent ($D$) of rhodamine within experimental error (Table 2), consistent with the purported deep penetration of the peptide (Fig. 2) and its small surface effects (Figs 2 and 5, and Table 1). Melittin and magainin, however, reduced the diffusion rate of Rhodamine Red-DHPE (Table 2). This result confirms that binding of the two peptides to vesicles containing negatively charged phospholipids gives rise to significantly reduced mobility [48]. The lower diffusion coefficients induced by melittin and magainin are, similarly, consistent with the slower SR of Patman observed after addition of the two peptides to $Ole_2$PtdSer/PamOlePtdCho/PDA vesicles (Table 1). Accordingly, the fluorescence correlation spectroscopy data indicate that lipid binding of magainin and melittin decrease the lateral mobility of the phospholipids, which might be a consequence of a more rigid phospholipid headgroup region. KAL, on the other hand, did not affect the lateral mobility, as this peptide inserted deep into the bilayer.

The variations observed among the peptides in the SR experiments were more pronounced compared with the fluorescence correlation spectroscopy data and are related to fundamental differences between the biophysical parameters measured by the two techniques. Specifically, SR evaluates the changes in viscosity and micropolarity around the fluorescent label at a certain position within the bilayer, while fluorescence correlation spectroscopy experiments essentially determines the lateral diffusion coefficient (which, unlike SR values, is not a spectroscopically derived parameter) of a labeled phospholipid within the bilayer matrix.

**Table 2. Diffusion coefficients measured in the fluorescence correlation spectroscopy experiment of Rhodamine Red$^{TM}$–X-1,2-dihexadecanoyl-*sn*-glycero-3-phosphoethanolamine, triethylammonium salt (Rhodamine Red-DHPE) incorporated within $Ole_2$PtdSer/PamOlePtdCho (1 : 4 molar ratio) bilayers adsorbed onto a mica surface.** As demonstrated previously [46], the relative errors in the diffusion coefficients recorded in bilayers adsorbed onto mica surfaces, as determined using the 'z-scan' method, are ± 0.1. KAL, peptide sequence KKA(LA)7KK.

| Peptide added | Diffusion coefficient ($D$) ($\times 10^{-12}$ m$^2$·s$^{-1}$) |
|---|---|
| None | 3.9 |
| KAL | 4.0 |
| Melittin | 3.4 |
| Magainin | 3.2 |

## Quenching of the fluorescence of a lipid surface probe

The SR and fluorescence correlation spectroscopy measurements provided important information regarding the dynamic effect of the peptides interacting with the vesicles. We subsequently carried out a time-resolved fluorescence quenching experiment employing the fluorescent dye, NBD-PE, incorporated within the phospholipid/PDA vesicles (Fig. 6). The fluorescent NBD label in NBD-PE is localized in close proximity to the lipid headgroup–water interface and thus is a sensitive probe for surface perturbations by membrane-active species [49]. The fluorescence quenching data in Fig. 6 complement the colorimetric and SR data discussed above (Figs 2 and 5), providing an insight into dynamic processes, such as lipid flip-flop [17], closer to the bilayer surface, and further highlight the distinct behavior of the peptides in the two models examined. Figure 6 again demonstrates that differences in the quenching kinetics were apparent both among the peptides, as well as between the zwitterionic vs. negatively charged phospholipid-containing vesicles. Faster fluorescence quenching of NBD-PE was induced by all peptides in PamOlePtdCho/PDA vesicles (Fig. 6, ◆), compared with $Ole_2$PtdSer/PamOlePtdCho/PDA vesicles (Fig. 6, □). This result indicates a more pronounced interfacial perturbation induced by the peptides when the lipid bilayer contained only zwitterionic phospholipids, and is consistent with the observations, discussed above,

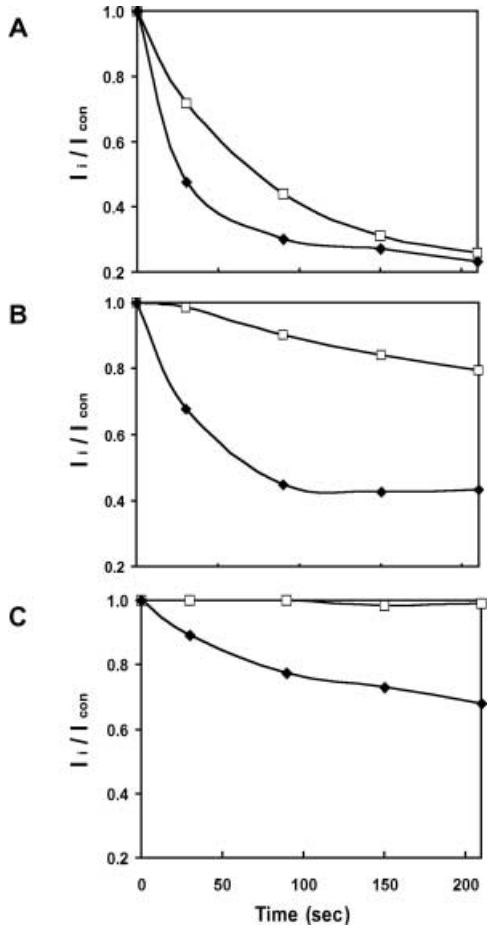


**Fig. 6. Time-resolved fluorescence quenching of NBD-PE.** Decay of the fluorescence (538 nm) of NBD-PE dye induced by sodium dithionite following addition of peptides. Data showing dithionite-induced quenching of fluorescence emission after addition of peptides relative to the control (no peptides added). Vesicles examined were NBD-PE/PamOlePtdCho/poly(diacetylene) (PDA) (0.2 : 2 : 3, molar ratio) (◆); NBD-PE/$Ole_2$PtdSer/PamOlePtdCho/PDA (0.2 : 1 : 1 : 3 molar ratio) (□). (A) Magainin; (B) melittin; (C) peptide sequence KKA (LA)7KK (KAL). Vesicle-bound concentrations of all peptides were 1 μM.

in the colorimetric experiments (Fig. 2), the time-dependent Stokes shifts of Patman (Table 1), and the SR experiments (Fig. 5).

The relative extent of fluorescence quenching induced by each peptide (Fig. 6) echoes the colorimetric and SR data. Magainin, for example, induced the fastest quenching among the three peptides in both vesicle models (Fig. 6A), probably reflecting its pronounced lipid–water interface binding and interactions. The hydrophobic sequence KAL, on the other hand, seemed to affect the fluorescence quenching to a much lesser degree compared with magainin and melittin (Fig. 6C). For example, in PamOlePtdCho/PDA vesicles, the NBD fluorescence decreased, within 60 s, to 60% after addition of magainin (Fig. 6A), but the corresponding value following KAL interaction was only ≈20% (Fig. 6C). The effect of KAL seemed particularly negligible in the $Ole_2$PtdSer/PamOlePtdCho/PDA assembly (Fig. 6C). This result could again be explained by the deep insertion of the hydrophobic helical peptide into the core of the bilayer, rather than localization at the charged lipid headgroup environment, which is the probable situation for magainin. Melittin induced an intermediate effect upon the fluorescence decay between KAL and magainin (Fig. 6B), which correlated with its lipid interaction profile inferred from the colorimetric and fluorescence experiments discussed above.

## Discussion

Elucidating the extent of bilayer penetration by membrane-active peptides and their effect upon lipid microenvironments and dynamics are crucial for understanding their biological activities. A limited number of reports, however, have examined in molecular detail the localization of membrane peptides within lipid bilayers. In this work we employed a multiprong approach, using colorimetric and fluorescence techniques applied in a biomimetic lipid–PDA platform, for evaluating the permeation profiles and dynamic effects of representative membrane-active peptides. The spectroscopic analysis points to distinct differences in penetration depth and bilayer localization among the three peptides. Furthermore, the results indicate that negatively charged phospholipids within lipid bilayers play prominent roles in promoting peptide binding and insertion into the membrane.

The experiments described here utilized phospholipid/PDA aggregates, which allow evaluation of relative peptide penetration into bilayers through measuring the concentration dependence of quantifiable blue–red transitions induced by membrane-associated peptides. The colorimetric data (Fig. 2) indeed suggest that interactions of the peptides were primarily interfacial in bilayers consisting solely of zwitterionic lipids, while deeper insertion of the peptides occurred when negatively charged phospholipids were also embedded in the bilayer. A similar picture emerged from the SR experiments (Fig. 5). Very small changes in the SR of the fluorescent dye Patman, located within the glycerol moieties of PamOlePtdCho bilayers, were induced by the peptides (Fig. 5A). However in vesicles containing negatively charged phospholipids ($Ole_2$PtdSer/PamOlePtdCho/PDA, Fig. 5B) SR times increased much more substantially (Table 1). The fluorescent quenching experiments by water-soluble dithionite (Fig. 6), in which the fluorescence of the NBD-PE probe displayed at the lipid headgroup–water interface decreased faster in the PamOlePtdCho/PDA vesicles in comparison to $Ole_2$PtdSer/PamOlePtdCho/PDA, were consistent with the surface localization of the peptides in the neutral lipid system.

Changes in the SR of fluorescent dyes incorporated in the headgroup region of bilayers are generally explained by two primary mechanisms: modification of the rigidity of the lipid environment in proximity to the fluorescent probe; and alteration of the amount and mobility of water molecules at the probe area [30,35,38]. The effects of the peptides on the SR in the two vesicle systems can be described in that framework, as follows: in the zwitterionic phospholipid bilayers, the peptides are primarily localized at the hydrophilic headgroup interface of the bilayer, thus

inducing small changes to the SR of Patman located more distantly in the bilayer; however, in the negatively charged phospholipid system, deeper penetration of the peptides would result in closer interactions between the peptides and the molecular environment of the probe, leading (through increased rigidity and ejection of water molecules) to longer SR times. Our data are also consistent with previous studies showing substantial retention of cytolytic peptides in membranes containing anionic lipids [5,11].

The fluorescence data also suggest that different mechanisms are responsible for the membrane-permeation properties of the examined peptides. Magainin displayed the most pronounced phospholipid interfacial effect, both in zwitterionic phospholipid vesicles as well as in vesicles containing negatively charged phospholipids. Melittin was less surface active than magainin in both systems, while the hydrophobic sequence, KAL, inserted deepest into the lipid hydrocarbon chain region, probably because of a predominant transmembrane orientation.

Combining the spectroscopic data for fluorophores incorporated at different bilayer environments allows evaluation of the proximate localization of the antimicrobial peptides within the different bilayer compositions. In the vesicles containing negative phospholipids, we observed that magainin was located close to the glycerol moieties (inferred from the SR measurements), while in the zwitterionic phospholipid vesicles, SR and NBD-PE fluorescence quenching measurements indicated significant peptide retention at the lipid–water interface. Indeed, it has been previously reported that magainins are highly sensitive to the lipid composition and can efficiently permeate only negatively charged bilayers [3,5]. Furthermore, magainin selectively targets bacterial species owing to exclusive abundance of the anionic lipids in the bacterial membrane [3,5,8]. Our findings suggest that insertion of magainin near the glycerol region might be directly related to its ability to disrupt anionic membranes and therefore is crucial for the antibacterial activity of the peptide. Similarly, the preferred incorporation of magainin at the lipid–water interface in the zwitterionic lipid bilayers might not induce membrane permeation, in agreement with the nonhemolytic properties of the peptide [4,5,8].

Melittin incorporates more deeply than magainin in the lipid bilayer, in all vesicle systems tested. This indicates that hydrophobic interactions play an important role in the peptide affinity to the membrane. The ability of melittin to permeate to the inner leaflet of the bilayer provides the basis for non-cell-selective toxicity of the peptide [3,4,8]. Differences in the depth of bilayer penetration between magainin and melittin, demonstrated in this study, provide further insights into the distinct modes of action of antibacterial peptides and toxins. The experiments also suggest that an important determinant in antimicrobial peptide action involves reduction of the mobility within lipid headgroup domains, which would explain the significant increase in the SR times following peptide–membrane interactions. Overall, our data imply that the 'carpet model', which points to bilayer-surface preorganization of antimicrobial peptides, is an important component in the mechanisms of antimicrobial peptides, and confirm the significance of amphipathic interactions of antimicrobial peptides to their biological activities.

## Acknowledgements

R.J. is grateful to the Israel Science Foundation for financial support. R.J. is a member of the Ilse Katz Center for Nano- and Meso-Science and Technology. J.S., A.B., and M.H. thank the Ministry of Education, Youth and Sports of the Czech Republic (via LN 00A032) for financial support.

## References

1. Zasloff, M. (2002) Antimicrobial peptides of multicellular organisms. *Nature* **415**, 389–395.
2. Hancock, R.E. & Diamond, G. (2000) The role of cationic antimicrobial peptides in innate host defences. *Trends Microbiol.* **8**, 402–410.
3. Papo, N. & Shai, Y. (2003) Exploring peptide membrane interaction using surface plasmon resonance: differentiation between pore formation versus membrane disruption by lytic peptides. *Biochemistry* **42**, 458–466.
4. Shai, Y. (1999) Mechanism of the binding, insertion and destabilization of phospholipid bilayer membranes by α-helical antimicrobial and cell non-selective membrane lytic peptides. *Biochim. Biophys. Acta* **1462**, 55–70.
5. Matsuzaki, K. (1999) Why and how are peptide–lipid interactions utilized for self-defense? Magainins and tachyplesins as archetypes. *Biochim. Biophys. Acta* **1462**, 1–10.
6. Ojcius, D.M. & Young, J.D. (1991) Cytolytic pore-forming proteins and peptides: is there a common structural motif? *Trends Biochem. Sci.* **16**, 225–229.
7. Pouny, Y., Rapaport, D., Mor, A., Nicolas, P. & Shai, Y. (1992) Interaction of antimicrobial dermaseptin and its fluorescently labeled analogs with phospholipid membranes. *Biochemistry* **31**, 12416–12423.
8. Shai, Y. (2002) Mode of action of membrane active antimicrobial peptides. *Biopolymers (Pept. Sci.)* **66**, 236–248.
9. Wakamatsu, K., Takeda, A., Tachi, T. & Matsuzaki, K. (2002) Dimer structure of magainin 2 bound to phospholipid vesicles. *Biopolymers* **64**, 314–327.
10. Blondelle, S.E. & Houghten, R.A. (1991) Hemolytic and antimicrobial activities of twenty four individual omissions analogues of melittin. *Biochemistry* **30**, 4671–4678.
11. Lee, T.H., Mozsolits, H. & Aguilar, M.I. (2001) Measurements of the affinity of melittin for zwitterionic and anionic membranes using immobilized lipid bioensor. *J. Peptide Res.* **58**, 464–476.
12. Killian, J.A., Salemink, I., de Planque, M.R., Maurits, R.R., Lindblom, G., Koeppe, R.E. II & Greathouse, D.V. (1996) Induction of nonbilayer structures in diacylphosphatidylcholine model membranes by transmembrane α-helical peptides: importance of hydrophobic mismatch and proposed role of tryptophans. *Biochemistry* **35**, 1037–1045.
13. Zhang, Y.P., Lewis, R.N., Henry, G.D., Sykes, B.D., Hodges, R.S. & McElhaney, R.N. (1995) Peptide models of helical hydrophobic transmembrane segments of membrane proteins. 1. Studies of the conformation, intrabilayer orientation, and amide hydrogen exchangeability of Ac-K2-(LA) 12-K2-amide. *Biochemistry* **34**, 2362–2371.
14. Giacometti, A., Cirioni, O., Barchiesi, F., Del Prete, M.S. & Scalise, G. (1999) Antimicrobial activity of polycationic peptides. *Peptides* **20**, 1265–1273.
15. Zasloff, M., Martin, B. & Chen, H.C. (1988) Antimicrobial activity of synthetic magainin peptides and several analogues. *Proc. Natl Acad. Sci. USA* **85**, 910–913.

16. Ludtke, S.J., He, K., Heller, W.T., Harroun, T.A., Yang, L. & Huang, H.W. (1996) Membrane pores induced by magainin. *Biochemistry* **35**, 13723–13728.
17. Matsuzaki, K., Murase, O., Fujii, N. & Miyajima, K. (1996) Antimicrobial peptide, magainin 2, induced rapid flip-flop of phospholipids coupled with pore formation and peptide translocation. *Biochemistry* **35**, 11361–11368.
18. Ladokhin, A.S. & White, S.H. (2001) 'Detergent-like' permeabilization of anionic lipid vesicles by melittin. *Biochim. Biophys. Acta* **1514**, 253–260.
19. Ladokhin, A.S., Selsted, M.E. & White, S.H. (1997) Sizing membrane pores in lipid vesicles by leakage of co-encapsulated markers: pore formation by melittin. *Biophys. J.* **72**, 1762–1766.
20. Yang, L., Harroun, T.A., Weiss, T.M., Ding, L. & Huang, H.W. (2001) Barrel-stave model or toroidal model? A case study on melittin pores. *Biophys. J.* **81**, 1475–1485.
21. Kolusheva, S., Kafri, R., Katz, M. & Jelinek, R. (2001) Cororimetric detection of interactions between antibodies and epitopes displayed at a biomimetic membrane interface. *J. Am. Chem. Soc.* **123**, 417–422.
22. Okada, S., Peng, S., Spevak, W. & Charych, D. (1998) Color and chromism of polydiacetylene vesicles. *Acc. Chem. Res.* **31**, 229–239.
23. Jelinek, R. & Kolusheva, S. (2001) Polymerized lipid vesicles as colorimetric biosensors for biotechnological applications. *Biotechnol. Adv.* **19**, 109–118.
24. Evrard, D., Touitou, E., Kolusheva, S., Fishov, Y. & Jelinek, R. (2001) Colorimetric screening of penetration enhancers using phospholipid/PDA asaemblies. *Pharm. Res.* **18**, 943–949.
25. Kolusheva, S., Shahal, T. & Jelinek, R. (2000) Cation-selective color sensors composed of ionophore-phospholipid-polydiacetylene mixed vesicles. *J. Am. Chem. Soc.* **122**, 776–780.
26. Kolusheva, S., Shahal, T. & Jelinek, R. (2000) Peptide–membrane interactions studied by a new phospholipid/polydiacetylene colorimetric vesicle assay. *Biochemistry* **39**, 15851–15859.
27. Kolusheva, S., Boyer, L. & Jelinek, R. (2000) A colorimetric assay for rapid screening of antimicrobial pepties. *Nat. Biotechnol.* **18**, 225–227.
28. Kolusheva, S., Wachtel, E. & Jelinek, R. (2003) Biomimetic/lipid polymer colorimetric membranes: molecular and cooperative properties. *J. Lipid Res.* **44**, 65–71.
29. Satchell, D.P., Sheynis, T., Shirafuji, Y., Kolusheva, S., Ouellette, A.J. & Jelinek, R. (2003) Interactions of mouse paneth cell α-defensins and α-defensin precursors with membranes: prosegment inhibition of peptide association with biomimetic membranes. *J. Biol. Chem.* **278**, 13838–13846.
30. Hof, M. (1999) Solvent relaxation in biomembranes. In *Applied Fluorescence in Chemistry, Biology, and Medicine* (Rettig, W., ed.), pp. 439–456. Springer-Verlag, Berlin.
31. Lakowicz, J.R. (1999) *Principles of Fluorescence Spectroscopy*, 2nd edn. Kluwer Academic/Plenum Publishers, New York.
32. Hutterer, R., Schneider, F.W., Lanig, H. & Hof, M. (1997) Solvent relaxation behaviour of n-anthroyloxy fatty acids in PC-vesicles and paraffin oil: a time-resolved emission spectra study. *Biochim. Biophys. Acta* **1323**, 195–207.
33. Hutterer, R., Parusel, A. & Hof, M. (1998) Solvent relaxation of prodan and patman: a useful tool for the determination of polarity and rigidity changes in membranes. *J. Fluorescence* **8**, 389–393.
34. Hutterer, R. & Hof, M. (2001) Anthroyloxy fatty acids: a unique set of fluorescent probes for the investigation of membrane structure and dynamics. *Recent Res. Dev. Lipids* **5**, 71–83.
35. Sykora, J., Kapusta, P., Fidler, V. & Hof, M. (2002) On what time scale does solvent relaxation in phospholipid bilayers happen? *Langmuir* **18**, 571–574.
36. Hutterer, R., Schneider, F.W., Sprinz, H.M. & Hof, M. (1996) Binding and relaxation behaviour of prodan and patman in phospholipid vesicles: a fluorescence and 1H NMR study. *Biophys. Chem.* **61**, 151–160.
37. Hutterer, R., Schneider, F.W. & Hof, M. (1997) Time-resolved emission spectra and anisotropy profiles for symmetric diacyl- and dietherphosphatidylcholines. *J. Fluorescence* **7**, 27–33.
38. Hutterer, R., Schneider, F.W., Hermens, W.T., Wagenvoord, R. & Hof, M. (1998) Binding of prothrombin and its fragment 1 to phospholipid membranes studied by the solvent relaxation technique. *Biochim. Biophys. Acta* **1414**, 155–164.
39. Chattopadhyay, A. & London, E. (1988) Spectroscopic and ionization properties of *N*-(7-nitrobenz-2-oxa-1,3-diazol-4-yl)-labeled lipids in model membranes. *Biochim. Biophys. Acta* **938**, 24–34.
40. White, S.H., Wimley, W.C., Ladokhin, A.S. & Hristova, K. (1998) Protein folding in membranes: determining energetics of peptide–bilayer interactions. *Methods Enzymol.* **295**, 62–87.
41. Jelinek, R., Okada, S., Notvez, S. & Charych, D. (1998) Interfacial catalysis by phospholipases at conjugated lipid vesicles: colorimetric detection and NMR spectroscopy. *Chem. Biol.* **5**, 619–629.
42. Fee, R.S. & Maroncelli, M. (1994) Estimation of time zero spectrum in time-resolved emission measurements of solvation dynamics. *Chem. Phys.* **183**, 235–247.
43. Siano, D.B. & Metzler, D.E. (1969) Band shapes of the electronic spectra of complex molecules. *J. Chem. Phys.* **51**, 1856–1861.
44. Horng, M.L., Gardecki, J.A., Papazyan, A. & Maroncelli, M. (1995) Subpicosecond measurements of polar solvation dynamics: Coumarin 153 revisited. *J. Phys. Chem.* **99**, 17311–17337.
45. Benes, M., Billy, D., Hermens, W.T. & Hof, M. (2002) Muscovite (mica) allows the characterisation of supported bilayers by ellipsometry and confocal fluorescence correlation spectroscopy. *Biol. Chem.* **383**, 337–341.
46. Benda, A., Benes, M., Marecek, V., Lhotsky, A., Hermens, W.T. & Hof, M. (2003) How to determine diffusion coefficients in planar phospholipid systems by confocal fluorescencecorrelation spectroscopy. *Langmuir* **19**, 4120–4126.
47. Katz, M., Tsubery, H., Fridkin, M., Kolusheva, S., Shames, A. & Jelinek, R. (2003) Membrane interactions of polymyxin B derivatives studied by a lipid/polydiacetylene colorimetric assay. *Biochem. J.* **375**(Pt2), 405–413.
48. Pramanik, A., Thyberg, P. & Rigler, R. (2000) Molecular interactions of peptides with phospholipid vesicle membranes as studied by fluorescence correlation spectroscopy. *Chem. Phys. Lipids* **104**, 35–47.
49. McIntyre, J.C. & Sleight, R.G. (1991) Fluorescence assay for phospholipid membrane asymmetry. *Biochemistry* **30**, 11819–11827.